Digital in-line holography and the photonic jet method: routines and graphical user interfaces to generate numerical standards with the Lorenz-Mie theory

F. R.A. Onofri, Fabrice Lamadie

Digital in-line holography and the photonic jet method: routines and graphical user interfaces to generate numerical standards with the Lorenz-Mie theory

Fabrice R.A. Onofri[1,*], Fabrice Lamadie[2]
1 : Aix-Marseille University, CNRS, IUSTI, UMR 7343, Marseille, France
2 : CEA, DES, ISEC, DMRC, Univ Montpellier, 30207 Bagnols-sur-Ceze, Marcoule, France
* Correspondent author: fabrice.onofri@univ-amu.fr

Keywords: Holography, Lorenz-Mie theory, Computation, Particle, Size, Composition

ABSTRACT

A set of MATAB® routines and a graphical user interface (GUI) to model holograms of homogeneous, coated and multilayered particles are introduced. Based, on Lorenz-Mie theory, they are thought to be useful to the community working on the characterization of multiphase flows with Digital In-line Holography (DIH). Likewise, they can be used for the development of alternative approaches requiring numerical standards to evaluate their accuracy.

1. Introduction

DIH is a volumetric imaging technique allowing measuring the 3D position, dynamics, shape, and size of flowing micrometer- to millimeter-sized particles (e.g., bubbles, droplets, biological cells, aggregates, colloids, etc.)(Goodman, 1960; Hinsch & Herrmann, 2004; Pan & Meng, 2003; Sentis, Onofri, & Lamadie, 2018; Thompson, 1974). Despite its success, hologram processing times are still penalizing, and the resolution obtained on the particle axial position and particle size are not always sufficient. Furthermore, when operated as an imaging technique, conventioal DIH processing schemes does not provide any information on the particle composition, which is a critical parameter for many fields of research and industrial.

Basically, there exit two types of approaches - direct and inverse - to retrieve the particle field properties from recorded holograms. The first approach, called 'back-propagation', is a direct approach where the whole recorded hologram is back-propagated with diffraction integrals to obtain in focus 2D images of all the particles within the probe volume (Dubois, Schockaert, Callens, & Yourassowsky, 2006; Memmolo, Paturzo, Javidi, Netti, & Ferraro, 2014; Pan & Meng, 2003; Sentis, Bruel, Charton, Onofri, & Lamadie, 2017). The particle properties are determined by image processing techniques, and thus limited by the corresponding issues (threshold criteria and pixel size). But this approach does not require any assumption on the particle morphology and composition. The second approach, called 'regularization', is an inverse approach where the

particle properties are inferred thanks to a complex minimization process between experimental and numerically simulated holograms, e.g. (Jolivet et al., 2018; Mallery & Hong, 2019; Méès et al., 2013). This approach requires much more computational resources than the direct one. It demands also a particle model as one of the regularization inputs. Yet, its resolution in terms of particle axial position and particle size is potentially higher because it is not intrinsically limited by the pixel size in the particle plane. In some specific cases, this inverse approach can also infer the phase of the hologram (Latychevskaia, 2019) as well as the particle refractive index (Lee et al., 2007). For large particles, the particle model is a simple opaque disk propagated with diffraction integrals, while for micrometer particles data base of holograms computed with electromagnetic light scattering theories are preferred, e.g. (Lee et al., 2007; Wu et al., 2012). In practice, it turns out that the inverse approach is limited to the characterization of simple objects in dilute flows, while direct approach can handle more complex particle shape and flows (like sprays with deformed droplets and ligaments for instance, e.g. (Gao et al., 2013)).

The present authors have recently proposed to analyze the photonic jet (also called Airy disk or caustic spot), formed by large spherical, transparent and homogeneous particle (see Fig. 1). It allows to enhance DIH capabilities in terms of particle axial location, in free space (Sentis, Onofri, & Lamadie, 2017; Sentis et al., 2018) or in pipe flows (Sentis, Bruel, et al., 2017), as well as for particle material recognition (Sentis, Onofri, et al., 2017; Sentis et al., 2018). This method is an hybrid approach coupling holograms back-propagation and processing analyze assuming a particle model. In pioneer works (Choi & Lee, 2011; Sentis, Bruel, et al., 2017; Sentis, Onofri, et al., 2017; Tian, Gao, & Barbastathis, 2011) the particle model was a simple geometrical optics approximation only valid within the paraxial limit. But the concept of the method was also tested and proven with physical Optics (Sentis et al., 2018) and electromagnetic calculations (Sentis, Bruel, et al., 2017; Sentis, Onofri, et al., 2017), together with experiments carried on drops, bubbles and glass spheres (Sentis et al., 2018). To go further in this process, and make DIH technique fully applicable, by reducing its computation time and improving its resolution, the development of more sophisticated particle models as well as the availability of numerical standards are thought to be fundamental. And this, whether a direct or inverse approach is employed to process the holograms.

In this perspective, this paper presents a work in progress on the development of numerical tools allowing to produce hologram standards and analyse the particle near-field characteristics. Following this introduction, section 2 summarizes the mathematical and physical background of

the numerical routines developed, while section 3 presents the GUI (called '**DIHMie 1.1.** ') implemented under Matlab® environment. Section 4 provides some examples that illustrate the capabilities and possible applications of these numerical tools. Section 5 is an overall conclusion.

2. Electromagnetic standards of holograms of homogeneous, coated and multilayred particles

2.1 Lorenz-Mie calculations

The routines implemented to model holograms with the Lorenz-Mie theory (LMT) are based on previous Fortran codes developed by Barber and Hill (Barber & Hill, 1990) for homogeneous spheres and that were translated in MATLAB® and extended to coated and multilayer spheres by Onofri et al. (Onofri, Gréhan, & Gouesbet, 1995) .

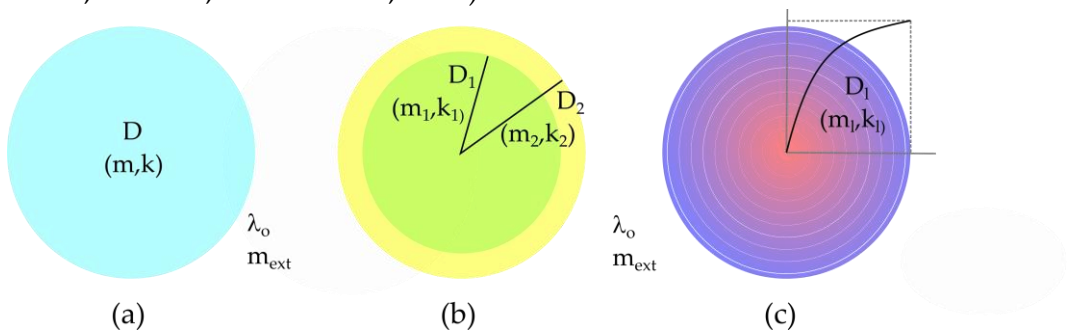

Fig. 1 Particle morphologies taken into account: homogeneous, coated and multilayered spheres.

In this model, the three components (r,θ,ϕ) of the incident electrical field $E_r^{inc}, E_\theta^{inc}, E_\phi^{inc}$, from a linear or non-polarized incident plane wave, as well as the internal $E_r^{\text{int}}, E_\theta^{\text{int}}, E_\phi^{\text{int}}$ and scattered $E_r^{sca}, E_\theta^{sca}, E_\phi^{sca}$ electrical fields are calculated with series of Legendre's polynomials, Bessel and Hankel functions (Barber & Hill, 1990; Bohren & Huffman, 1998; Onofri et al., 1995).

These series are truncated for expansion parameters such as $n \geq n_{stop}$ (Wiscombe, 1980), with $n_{stop} = INT(\alpha_{stop}) + 1$ where $\alpha = \pi D/\lambda$ stands for the particle size parameter in the considered medium (refractive index m_{ext}) and for the incident wavelength in the embedding medium $\lambda = \lambda_0 / m_{ext}$, with

$$\begin{aligned} \alpha_{stop} &= \alpha + 4\alpha^{1/3} + 1, \; for \; \alpha \in \left[0.02, 8\right] \\ \alpha_{stop} &= \alpha + 4.05\alpha^{1/3} + 2, \; for \; \alpha \in \left]8, 4200\right] \\ \alpha_{stop} &= \alpha + 4\alpha^{1/3} + 2, \; for \; \alpha \in \left]4200, 20000\right] \end{aligned} \tag{0.1}$$

The particle properties are their 3D coordinates $(x,y,z)_p$ with respect to a laboratory coordinate system $(Oxyz)$, a single complex refractive index (m,k) and diameter D for homogeneous spheres,

two complex refractive indices $(m_1,k_1;m_2,k_2)$ and two diameters (D_1,D_2) for coated spheres and a single diameter with up to typically $L=5000$ complex refractive indices $(m_\ell,k_\ell;\ell=1,2,\cdots L)$ for radially inhomogeneous spheres, see Fig. 1. The calculations can be sequential or parallel (on the CPU workers). Basically, the main output is the intensity of the electromagnetic field on a plane $(x,y,z)_c$ mimicking the surface of the CCD sensor that is perpendicular to z-axis and at located at distance z_c from the laboratory coordinate center. The CCD sensor, quadratic, is defined by its pixels size and number. The considered electromagnetic field can be either the incident (reference wave) or, more interesting, the scattered or the total (scattered plus incident) field of a single particle or a cloud of n_p particles $(D,m,k,x,y,z)_p$. For a cloud of particles, the routines allow accounting for the interferences between the fields scattered by all particles as if their where alone. However, classically, the perturbation of the incident wave by each particle is not taken into account, in other words a dilute (or single scattering) optical regime is assumed.

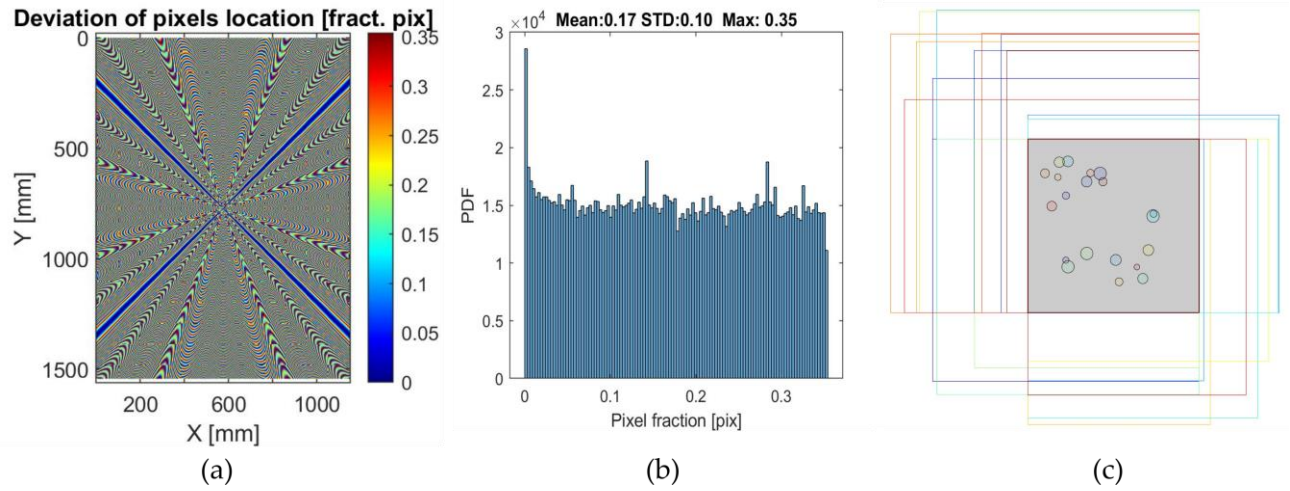

Fig. 2 Some windows of DIHMie 1.1. (a-b) Residual error on the true pixel location for an interpolation increment of 0.5 pixel: (c) Chart exemplifying all individual particle (colored disks) location and corresponding holograms to be calculated (boundaries in color) to retrieve the total field generated on the CCD sensor (area filled in gray).

2.2 Interpolation method and asymptotic approximation to speed up electromagnetic calculations

Even with the parallelization option, the calculations can be rather lengthy for high resolution holograms of large particles, and more specially when the particles are far from the CCD sensor. The latter limitation comes from the difficulty to calculate accurately the Hankel functions at large distances from the particle. To reduce the computational efforts, four solutions have been

implemented. They allow to reduce significantly the total computational time without noticeable loss of precision (see **Fig. 2** and **Fig. 4**):

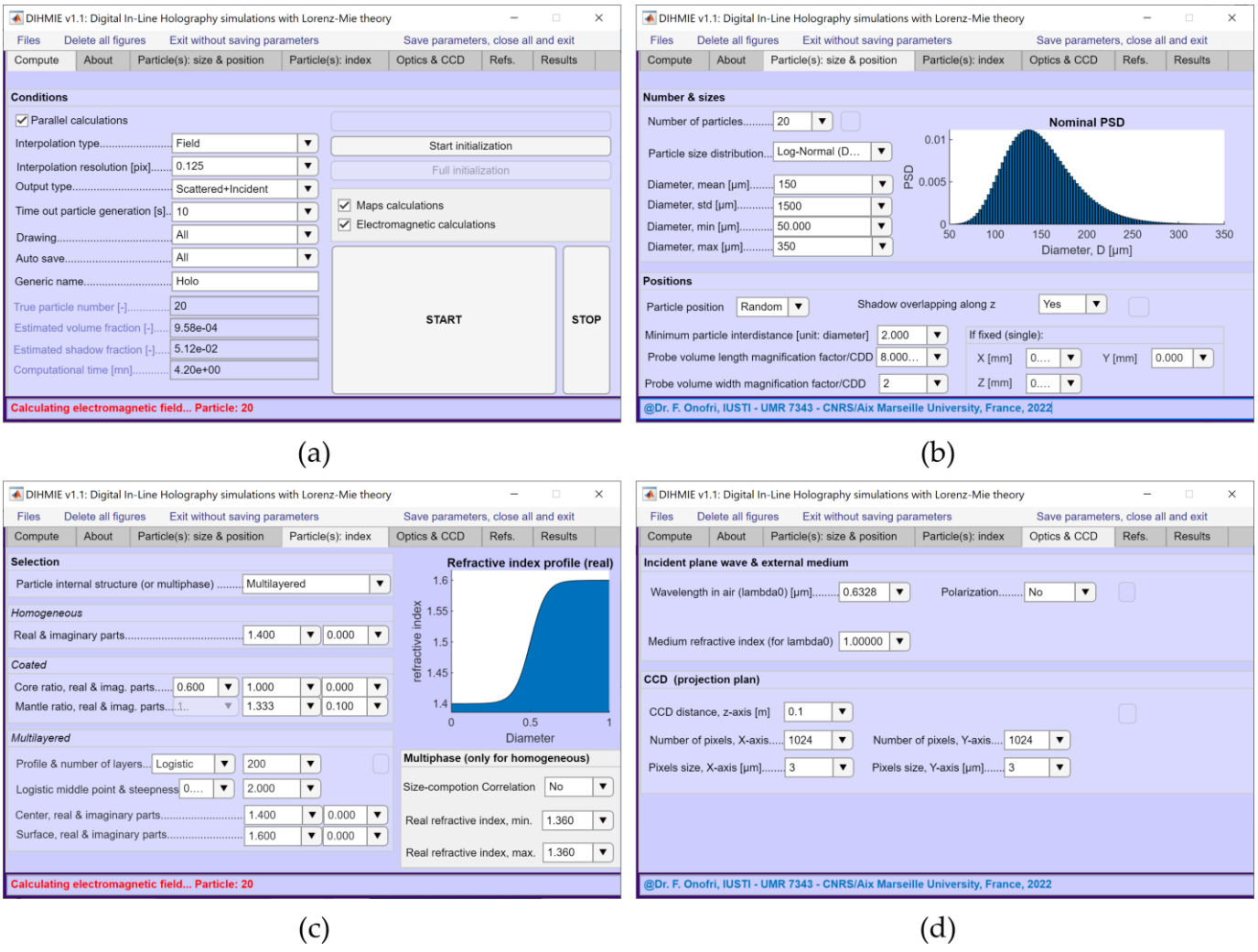

Fig. 3 Main windows of the GUI **DIHMie 1.1** under Matlab® environement: (a) Selection of the electromagnetic output type (e.g. incident, scattered, full field), resolution of the interpolation scheme, excecution and stop...; (b) Parameters of the particle characteristic distribution in size and in space...; (c) Particle model (homogeneous, coated or multilayered) and refractive index...; (d) Incoming light characteristics and CCD specification...

- First, for large distances, the calculation of the Hankel function is performed with asymptotic expressions (Abramowitz & Stegun, 1965) rather than downward recurrences.

- Second, since the hologram of rotationally symmetric particles is also rotationally symmetric, a special numerical scheme was developed to interpolate the electromagnetic field componenetson the whole sensor surface from its values calculed along the CCD sensor diagonal. The latter is over sampled to improve accuracy in term of pixel location (i.e. scattering angle), see **Fig.** 2 a, b (and **Fig.** 4).
- Third, to account for the lateral shift of the particle coordinates $(x,y)_p$ with respect to the CCD coordinate system $(x,y)_c$, the electromagnetic calculations for each particle are performed only for the diagonal of the rectangle which overlasp with the CCD sensor area (see **Fig.** 2 c).
- Fourth, the three complex components of each electrical field are interpolated with a bilinear interpolation method prior to calculate with the Poynting's vector the local electromagnetic intensity.

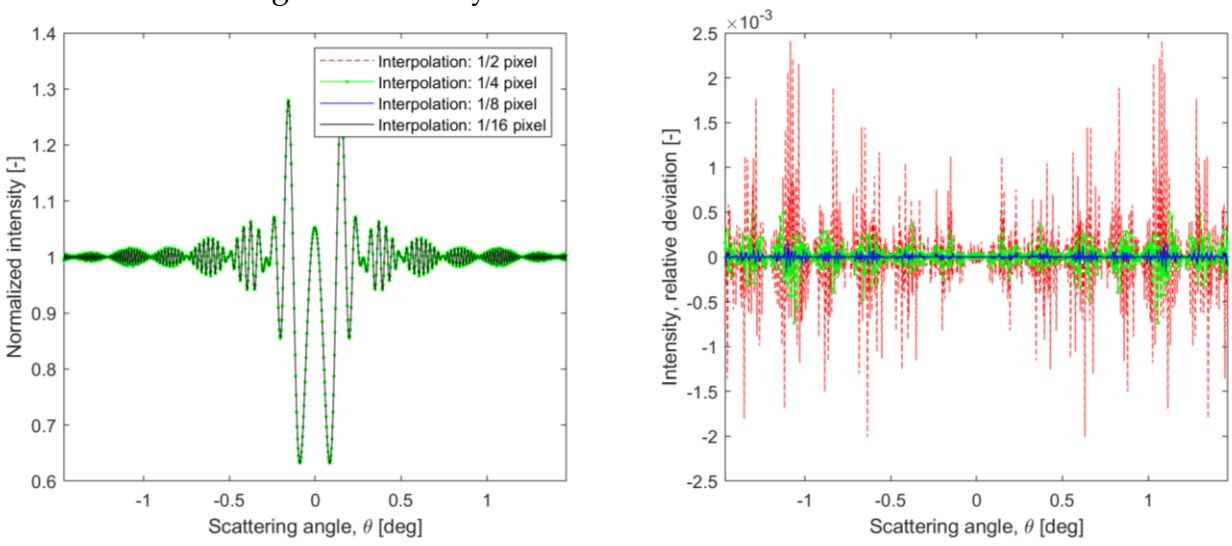

(a) (b)

Fig. 4 (a) Comparison of the radial intensity profile of the hologram of a water droplet in air, with diameter 125µm, versus the resolution of the interpolation method used to calculate the complex electromagnetic field across the whole CCD: 1/2, 1/4, 1/8 or 1/16 pixels. (b) corresponding relative error. Other parameters: $z_c = 0.1m$, pixels size and number: 5 x 5 µm^2 and 1024x1024 respectively, $\lambda_0 = 0.5\mu m$ λ_o=0.5µm, non polarized incident light.

3 Graphical user interface : "DIHMie", version 1.1.

All routines can be used independently, however a MATLAB® apps (called GUI here) was also developed for a more user-friendly usage, illustrated in **Fig. 3**. The first window (a) allows the user

to manage the calculations, select the interpolation resolution, the output type (scattered or total field), etc. The second window allows generating (or import) different types of particle size distributions, as well as the particle spatial distribution. The third window allows controling the particle material properties, while the fourth one allows to set the other parameters of the setup: CCD distance, pixel size and number,…

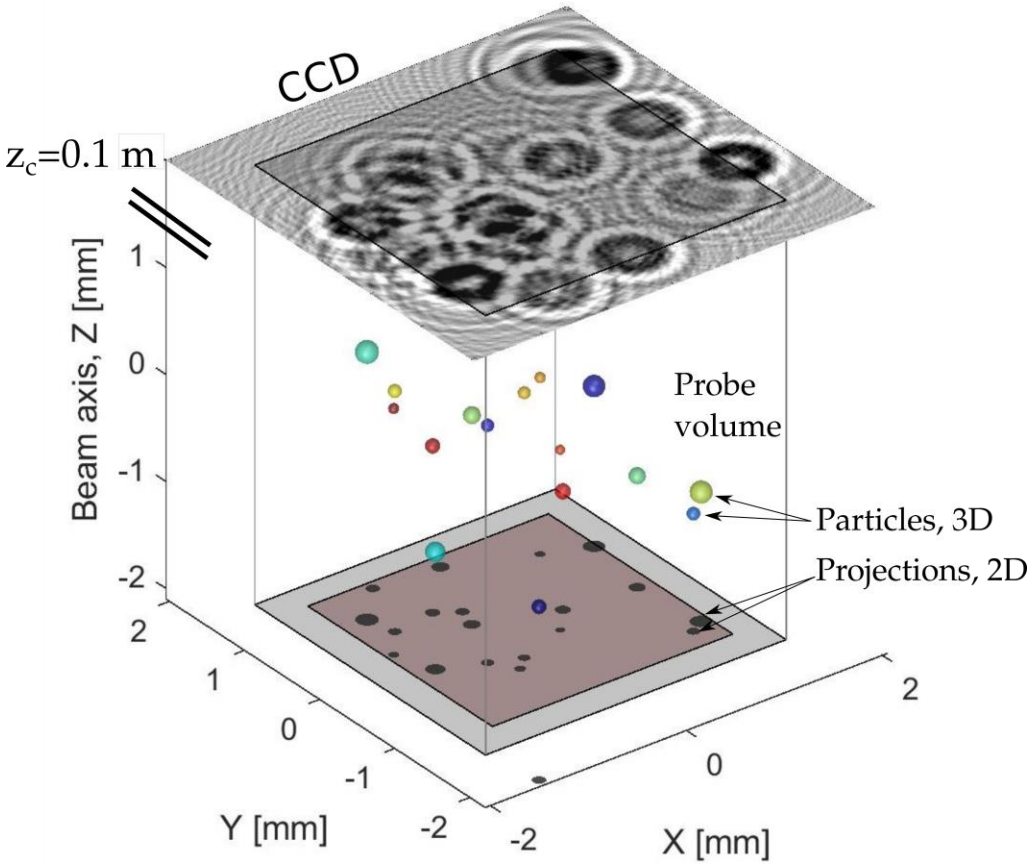

Fig. 5 Typical output of **DIHMie 1.1**: hologram produced by a cloud of $n_p = 20$ particles with a Log-Normal PSD (here, between 80 and 170µm). Same parameters than in Fig. 4. For drawing considerations,the hologram is drawn nearby the probe volume centre while it is located at a much larger distance $\left(z_c = 0.1m\right)$. The zone highlighted in red is used to control the particle lateral dispersion regarding the CCD area and calculate the particle concentration.

4. Example of results

The set of routines allows calculating hologram standards, as well as various quantities of interest for the development of DIH: intensity profile of the electromagnetic intensity in the Photonic jet region, the near-field intensity and electromagnetic field phase inside and around the particle, or in the whole xz-plane.

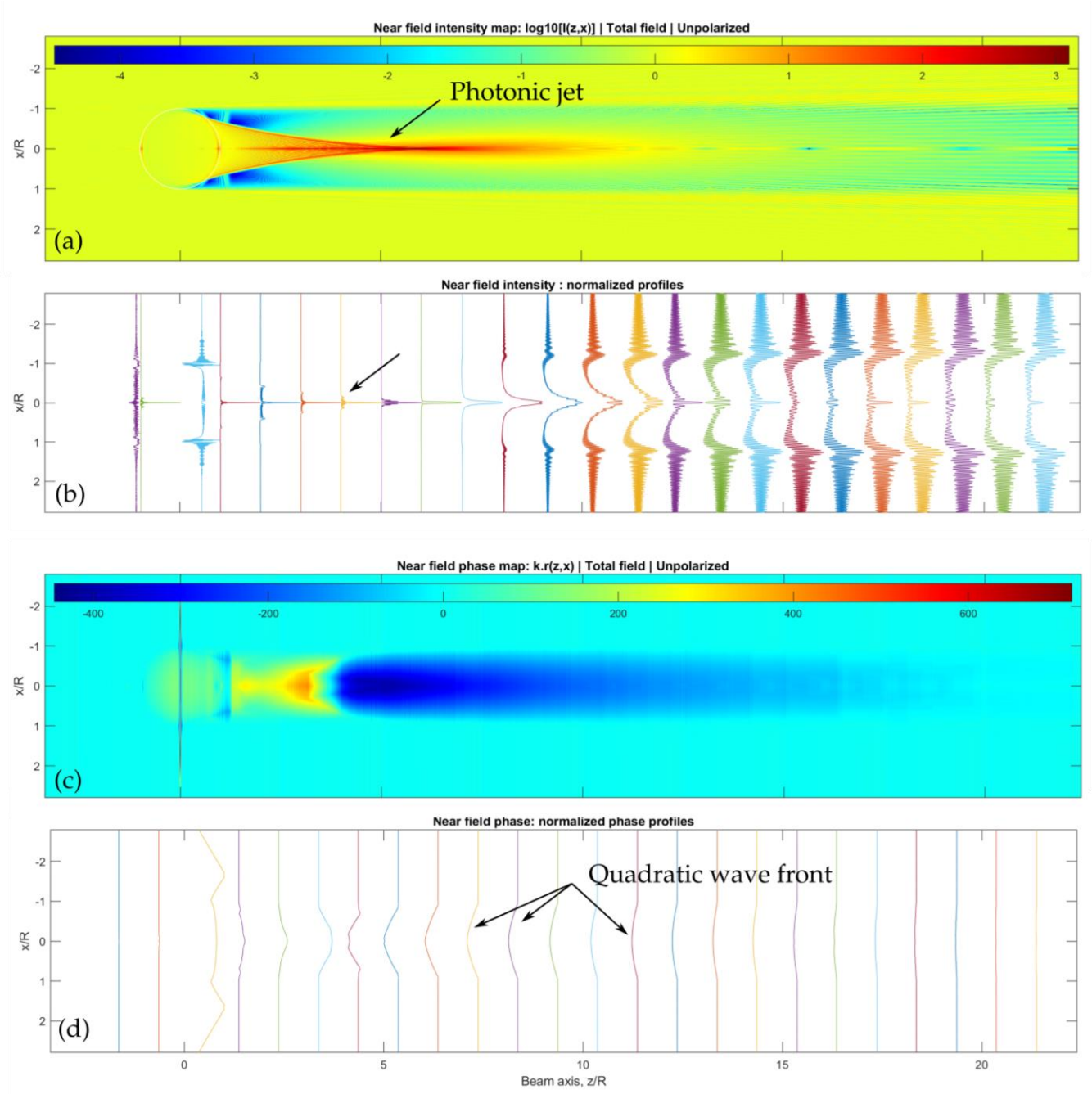

Fig. 6 Near field (a-b) intensity and (c-d) unwrapped phase inside and around an oil droplet (m_0=1.4437) in water (m_{ext}=1.3317) with diameter D=2R=125µm, illuminated by a plane wave (λ_0=0.532m, unpolarized).

The accuracy of the interpolation method for the hologram radial intensity profile can be evaluated from **Fig. 2** and **Fig. 4**. For the typical case considered here, a water droplet of 125µm observed at

10 cm with a high resolution CCD camera, the maximum deviation is only of 0.25% for an interpolation of 1/2 pixel, and 0.02% for 1/8 pixel.

A basic ouput of **DIHMie** 1.1 is illustrated with **Fig. 5** which shows a hologram produced by a cloud of $n_p = 20$ particles with a Log-Normal particle size distribution (PSD) randomly distributed in a probe volume with dimensions 3x3x8 mm^3. The particle projected area is used to assess the particle concentration $\left(C_v \approx 10^{-3}\right)$ as well as for illustrative purpose. This full hologram was obtained in 4 minutes with a labtop (Intel i7-10875H 2.3GHz 64 Go).

These routines allows also calculating other quantities of interest like the near-field intensity and phase inside and outside a single particle, see **Fig.** 6. The latter emphasizes on the extreme localisation and intensity of the photonic jet, as well as the quadratic shape of the diverging wave front (Duan, Onofri, Han, & Ren, 2021) generated by refracting droplet in the near-forward direction.

5. Conclusion

The numerical tools introduced in this paper allow the exact calculation of holograms standards as well as the electromagnetic near-field intensity and phase inside and outside a homogeneous, coated or multilayered sphere. Available from the corresponding author on reasonable request, they are are thought to be useful to the community working on the characterization of multiphase flows. Likewise, they can be used for the development of alternative approaches requiring numerical standards to evaluate their accuracy.

6. References

Abramowitz, M., & Stegun, I. A. (1965). *Handbook of mathematical Functions*. New-York: Dover inc.

Barber, S. C., & Hill, P. W. (1990). *Light Scattering by particles : computational methods*. London: World Scientific.

Bohren, C. F., & Huffman, D. R. (1998). *Absorption and scattering of light by small particles*. New york: Wiley & Sons.

Choi, Y.-S., & Lee, S.-J. (2011). High-accuracy three-dimensional position measurement of tens of micrometers size transparent microspheres using digital in-line holographic microscopy. *Optics Letters, 36*(21), 4167-4169. doi:10.1364/OL.36.004167

Duan, Q., Onofri, F. R. A., Han, X. e., & Ren, K. F. (2021). Generalized rainbow patterns of oblate drops simulated by a ray model in three dimensions. *Optics Letters, 46*(18), 4585-4588. doi:10.1364/OL.434149

Dubois, F., Schockaert, C., Callens, N., & Yourassowsky, C. (2006). Focus plane detection criteria in digital holography microscopy by amplitude analysis. *Optics Express, 14*(13), 5895-5908. doi:10.1364/OE.14.005895

Gao, J., Guildenbecher, D. R., Reu, P. L., Kulkarni, V., Sojka, P. E., & Chen, J. (2013). Quantitative, three-dimensional diagnostics of multiphase drop fragmentation via digital in-line holography. *Optics Letters, 38*(11), 1893-1895. doi:10.1364/OL.38.001893

Goodman, J. W. (1960). Introduction to Fourier Optic. *Mac. Graw-Hill, New York*.

Hinsch, K. D., & Herrmann, S. F. (2004). Holographic Particle Image Velocimetry. *Measurement Science and Technology, 15*(4). doi:10.1088/0957-0233/15/4/e01

Jolivet, F., Momey, F., Denis, L., Méès, L., Faure, N., Grosjean, N., Fournier, C. (2018). Regularized reconstruction of absorbing and phase objects from a single in-line hologram, application to fluid mechanics and micro-biology. *Optics Express, 26*(7), 8923-8940. doi:10.1364/OE.26.008923

Latychevskaia, T. (2019). Iterative phase retrieval for digital holography: tutorial. *Journal of the Optical Society of America A, 36*(12), D31-D40. doi:10.1364/JOSAA.36.000D31

Lee, S.-H., Roichman, Y., Yi, G.-R., Kim, S.-H., Yang, S.-M., Blaaderen, A. v., Grier, D. G. (2007). Characterizing and tracking single colloidal particles with video holographic microscopy. *Optics Express, 15*(26), 18275-18282. doi:10.1364/OE.15.018275

Mallery, K., & Hong, J. (2019). Regularized inverse holographic volume reconstruction for 3D particle tracking. *Optics Express, 27*(13), 18069-18084. doi:10.1364/OE.27.018069

Méès, L., Grosjean, N., Chareyron, D., Marié, J.-L., Seifi, M., & Fournier, C. (2013). Evaporating droplet hologram simulation for digital in-line holography setup with divergent beam. *Journal of the Optical Society of America A, 30*(10), 2021-2028. doi:10.1364/JOSAA.30.002021

Memmolo, P., Paturzo, M., Javidi, B., Netti, P. A., & Ferraro, P. (2014). Refocusing criterion via sparsity measurements in digital holography. *Optics Letters, 39*(16), 4719-4722. doi:10.1364/OL.39.004719

Onofri, F., Gréhan, G., & Gouesbet, G. (1995). Electromagnetic scattering from a multilayered sphere located in an arbitrary beam. *Applied Optics, 34*(30), 7113-7124. doi:10.1364/ao.34.007113

Pan, G., & Meng, H. (2003). Digital holography of particle fields: reconstruction by use of complex amplitude. *Applied Optics, 42*(5), 827-833. doi:10.1364/AO.42.000827

Sentis, M. P. L., Bruel, L., Charton, S., Onofri, F. R. A., & Lamadie, F. (2017). Digital in-line holography for the characterization of flowing particles in astigmatic optical systems. *Optics and Lasers in Engineering, 88*, 184-196. doi:http://dx.doi.org/10.1016/j.optlaseng.2016.08.012

Sentis, M. P. L., Onofri, F. R. A., & Lamadie, F. (2017). Photonic jet reconstruction for particle refractive index measurement by digital in-line holography. *Optics Express, 25*(2), 867-873. doi:10.1364/OE.25.000867

Sentis, M. P. L., Onofri, F. R. A., & Lamadie, F. (2018). Bubbles, drops, and solid particles recognition from real or virtual photonic jets reconstructed by digital in-line holography. *Optics Letters, 43*(12), 2945-2948. doi:10.1364/OL.43.002945

Thompson, B. J. (1974). Holographic particle sizing techniques. *Journal of Physics E: Scientific Instruments, 7*(10), 781.

Tian, L., Gao, H., & Barbastathis, G. (2011, 2011/07/10). *Digital holographic imaging of multi-phase flows.* Paper presented at the Imaging and Applied Optics, Toronto.

Wiscombe, W. J. (1980). Improved Mie scattering algorithms. *Applied Optics, 19*(9), 1505-1509. doi:10.1364/AO.19.001505

Wu, X., Meunier-Guttin-Cluzel, S., Wu, Y., Saengkaew, S., Lebrun, D., Brunel, M., Grehan, G. (2012). Holography and micro-holography of particle fields: A numerical standard. *Optics Communications, 285*(13), 3013-3020. doi:https://doi.org/10.1016/j.optcom.2012.02.101